Review

María Taeño, David Maestre* and Ana Cremades

An approach to emerging optical and optoelectronic applications based on NiO micro- and nanostructures

https://doi.org/10.1515/nanoph-2021-0041
Received February 1, 2021; accepted April 20, 2021;
published online May 10, 2021

Abstract: Nickel oxide (NiO) is one of the very few *p*-type semiconducting oxides, the study of which is gaining increasing attention in recent years due to its potential applicability in many emerging fields of technological research. Actually, a growing number of scientific works focus on NiO-based electrochromic devices, high-frequency spintronics, fuel cell electrodes, supercapacitors, photocatalyst, chemical/gas sensors, or magnetic devices, among others. However, less has been done so far in the development of NiO-based optical devices, a field in which this versatile transition metal oxide still lags in performance despite its potential applicability. This review could contribute with novelty and new forefront insights on NiO micro and nanostructures with promising applicability in optical and optoelectronic devices. As some examples, NiO lighting devices, optical microresonators, waveguides, optical limiters, and neuromorphic applications are reviewed and analyzed in this work. These emerging functionalities, together with some other recent developments based on NiO micro and nanostructures, can open a new field of research based on this *p*-type material which still remains scarcely explored from an optical perspective, and would pave the way to future research and scientific advances.

Keywords: luminescence; nanostructures; nickel oxide; optical limiter; optical resonator; waveguiding behavior.

***Corresponding author: David Maestre**, Física de Materiales, Universidad Complutense de Madrid Facultad de Ciencias Físicas, Plaza de las Ciencias 1, Madrid, 28040, Spain,
E-mail: dmaestre@ucm.es. https://orcid.org/0000-0001-9898-2548
María Taeño and Ana Cremades, Física de Materiales, Universidad Complutense de Madrid Facultad de Ciencias Físicas, Plaza de las Ciencias 1, Madrid, 28040, Spain

1 Introduction

Among the very few *p*-type metal oxides, nickel oxide (NiO) stands out as one of the most promising candidates in diverse forefront fields of research owing to its singular physico-chemical properties. This transition metal oxide exhibits rock-salt structure with octahedral Ni^{2+} and O^{2-} sites. In this structure, nickel atoms occupy the corners of the cube and the centers of the faces, while oxygen atoms occupy the centers of the edges and the center of the cube, following the characteristic *fcc-packed* structure. The space group of NiO is, $Fm\bar{3}m$ with lattice parameters $a = b = c = 4.177$ Å [1]. It should be noted that at temperatures below the Néel temperature, this oxide can suffer a weak cubic-to-rhombohedral distortion (space group $R\bar{3}m$ and lattice parameters $a = b = 2.955$ Å and $c = 7.227$ Å) attributed to a magnetostriction effect [2]. NiO has a wide bandgap around 3.6–4.3 eV and exhibits excellent chemical stability, durability, low toxicity, high ionization energy, and low-cost processing as well as interesting electrical, optical, and magnetic properties [3]. Usha et al. [4] reported a detailed study of the most significant optical constants such as plasma resonance frequency (ω_p), refractive index (n), or dielectric constant (ε), in NiO thin films prepared by radio frequency magnetron sputtering technique. Table 1 shows the values of the optical parameters from NiO thin films calculated as a function of the radio frequency power.

Based on its characteristic nonstoichiometry, electronic band structure, spin configuration, and dimensionality this versatile oxide has demonstrated applicability in several fields of technological research. Considering experimental and theoretical results, it is well-known that Ni 3*d* states form the lowest conduction band states in NiO, while O 2*p* states mainly form the highest valence band states [5]. The electronic structure is mainly a result of hybridization of Ni 3*d* and O 2*p* in the NiO_6 octahedra [2]. Moreover, NiO is an antiferromagnetic electrically insulating material with resistivities up to 10^{13} Ω/cm in its stoichiometric form with a Néel temperature of 523 K [6].

Table 1: Values of dielectric constant (ε), refractive index (n), and plasma frequency (ω_p) from NiO, extracted from Ref. [4].

RF Power	ε	n	ω_p (s^{-1}) $\times 10^8$
100 W	1.754	1.676	2.13
150 W	2.040	1.905	4.43
200 W	2.676	2.114	4.61

However, its conductivity can be improved by increasing the concentration of nickel vacancies and oxygen interstitials, either by a controlled synthesis or by appropriate doping. For example, Napari et al. [6] reported the growth of NiO thin films following a plasma-enhanced atomic layer deposition, which were characterized by Hall effect measurements. The results showed resistivity values in a range between 80 and 200 Ω/cm as a function of the film thickness, measured using a van der Pauw configuration. These films were confirmed to have *p*-type conductivity, with a carrier concentration around 10^{17} cm^{-3} and mobility close to 0.1 cm^2/Vs. Following a similar procedure, Diao et al. [7], synthesized Li doped NiO thin films with different annealing temperatures and times by a modified spray method. Li doped NiO films exhibited a *p*-type conductivity with resistivities between 4.73 and 1.08 Ω/cm, carrier concentrations between 10^{14} and 10^{17} cm^{-3} and mobilities between 2.39 and 11.96 cm^2/Vs. The *p*-type behavior has been also observed in Sn-doped three dimensionally ordered macroporous NiO, as confirmed Wang et al. [8]. In this case, the carrier concentrations varied from 4.78×10^{16} to 8×10^{12} cm^{-3} and mobilities were found from 1.31 to 662.25 cm^2/Vs. For all the cases, the improvement in the conductivity is associated to a non-stoichiometry of NiO promoted by dopants incorporation and/or different synthesis conditions, which enhance the characteristic low conductivity of stoichiometric NiO. The origin of the *p*-type conductivity of NiO is related to the formation of interstitial oxygen [9, 10] and the inherent nickel deficiency, which motivates its extended use as hole transport material in optoelectronic devices. NiO, usually exhibits an oxygen excess accommodated by nickel vacancies. Both, theoretical and experimental results have shown that the formation energy of Ni vacancies is the lowest for all the defects, leading to *p*-type conduction [5, 6]. Moreover, the intrinsic nickel deficiency is usually accompanied by the formation of Ni^{3+} in order to reach charge neutrality [11]. The nickel vacancies created at the cation sites can be ionized to create Ni^{3+} following the reaction:

$$2Ni_{Ni}^{x} + 1/2\,O_2 \rightarrow 2Ni_{Ni} + O_O^x + V_{Ni}''$$

where two Ni^{2+} (Ni_{Ni}^{x}) react with oxygen to produce one ionized nickel vacancy (V_{Ni}'') and two Ni^{3+} (Ni_{Ni}) ions in the NiO crystal. Each created Ni^{3+} ion, acts as a donor which donates a hole, confirming the *p*-type conductivity of this oxide.

Over the last years, NiO micro and nanostructures have demonstrated significant applicability in a wide range of research fields, including spintronics, supercapacitors, fuel cell electrodes, photocatalysis, chemical gas sensors, or magnetic devices, among others [12–16]. The high transparency in the visible range of this wide band gap material, together with its large hole conductivity and high charge carriers mobility make NiO a suitable option for optoelectronic devices. Among these applications, NiO is recognized of prime choice in electrochromic devices and smart windows [17, 18], in which NiO is extensively used as anodic colouring material. The electrochromic behaviour of this transition metal oxide is based on the colour changes related to the variations in the oxidation state of the Ni ion under an applied bias. Over the last years, the use of this transition metal oxide in photovoltaic devices is attracting great interest as well. To date NiO is claimed to be a promising candidate to be used in emerging perovskite solar cells [19, 20], where it is mainly used as a hole transport layer. Besides, NiO has been also employed in *p*-type dye sensitized solar cells (DSSC) [21], in which the normal principle of the common *n*-type DSSC is inverted, as well as in tandem photovoltaic devices based on its combination with other *n*-type oxides [22]. Indeed, *p*–*n* heterojunction based on *p*-type NiO and well-known *n*-type oxides such as ZnO and TiO_2 have been also developed as photodiode heterojunctions with demonstrated applicability as photodetectors [23, 24]. Although *p*-type solar cells have been widely exploited, the maximum photoconversion efficiency (PCE) is still lower in comparison with other *n*-type semiconducting oxides such as SnO_2, ZnO or TiO_2 among others. For example, dye-sensitized solar cells (DSSCs) have reached a mature stage with PCE over 14% for *n*-type cells [25], while *p*-type DSSCs have reached moderate PCEs of up to 2.5% [26]. In this context, inorganic–organic halide perovskite solar cells (PSCs) have received attention in the last years due to the significant increase in power conversion efficiency, from 3.8% in 2009 to 25.2% recently [27]. In the interest of improvement of these devices, it is important to select an efficient hole transport layer material, being NiO one of the most studied *p*-type oxides. The large bandgap and the deep-lying valence band that cause favourable energy level alignment with the perovskite active layer, makes NiO a promising candidate for these devices [27]. Recently, Kim et al. [27] reported a photoconversion efficiency of a PSC with NiO deposited by thermal evaporation around 17% with open

circuit voltage 1.07 V, short circuit current density of 20.68 mA/cm^2 and a fill factor of 75.51%. To date, the use of NiO as hole transport material is replacing common organic compounds such as PEDOT:PSS, as the stability and hydrophobic nature of the former provides lower degradation under high temperature and ambient moisture conditions. Furthermore, increased attention is gained by the use of NiO as a hole transport material in quantum dot solar cells (QDSCs), as recently reported for QDSCs based on PbS, Si, and N doped carbon quantum dots, among others [28, 29].

It is remarkable that despite the appealing merits of NiO to be used in optical and optoelectronic applications, this versatile material still lags in performance in these fields of research. Actually, the number of research works reporting on NiO-based optical applications is scarce so far, although over the last years a growing number of high impact scientific research point out to the promising applicability of NiO in diverse optical devices. This interest gives birth to the development of emerging research lines based on the applicability of NiO low dimensional structures as an optical and optoelectronic material.

Some of the recent developments on NiO-optical devices are based on the inherent optical nonlinearities of this material, associated with d–d transition levels and oxygen deficiency [30, 31], while some other applications exploit the opto-electronic properties of NiO. However, there are optical approaches in which the use of NiO still remains less explored despite its potential applicability. New perspectives to develop optical power limiters, optical switches, ultrafast photonic devices, photodetectors, optical resonators, lighting devices, or waveguides based on NiO have been recently explored, thus confirming the great interest aroused by NiO in the optic and optoelectronic fields in which there is still room for improvement.

This review is focused on less explored and emerging optical and optoelectronic applications based on NiO micro- and nanostructures. Recent scientific works reporting on the promising applicability of NiO in light emitting diodes and lighting devices, optical resonators, waveguides, saturable absorbers, and neuromorphic applications, where dimensions, morphology, and composition, play a key role, are reviewed.

2 Synthesis of NiO micro- and nanostructures

The advent of novel NiO based optical devices requires to face scientific and technological challenges, as the controlled achievement of low dimensional NiO with specific dimensions, morphology, composition and physicochemical properties. In some cases, their development and integration in diverse optical and optoelectronic devices are yet not resolved. Reducing the size to the microscale and nanoscale often offers advantages and novel applicability for NiO by improving the properties and/or adding new ones, thus allowing to explore novel functionalities. Different approaches have been explored so far for the synthesis of NiO micro- and nanostructures in order to adequate its characteristics to the required performances, which usually demand NiO with improved conductivity, specific defects and impurity levels in the bandgap, as well as particular dimensions. Furthermore, the design of optical devices usually requires a high control of the morphology and size of the NiO micro- and nanostructures, which can be used as building blocks in diverse optical and optoelectronic devices. Either chemical or physical routes have been employed so far in order to achieve an improved functionality of this transition metal oxide. It is well-known that numerous synthesis techniques have been employed in the last decades to deposit NiO thin films. Among these, spin-coating [32], spray pyrolysis [33], thermal evaporation [27], RF sputtering [34], and DC reactive magnetron sputtering [35] have been commonly reported. By controlling experimental conditions such as oxygen flow rates, thickness of the deposited NiO films or doping processes, the most relevant physical properties of NiO can be tailored. The need to overcome the actual limitations of thin films for their implementation in some devices, has led to the search of new strategies and synthesis methods which allow to obtain low dimensional micro- and nanostructures. Hence, in addition of the extended synthesis of NiO in form of thin films, it has been only recently that more variable and complex morphologies have been also reported in response to modern technological demands. Low dimensional NiO in forms of nanorods, wires, belts, sheets, tubes, or more complex morphologies such as flower-like structures and microcrystals with grid-pattern surfaces have been fabricated by means of different techniques. For the fabrication of the NiO nanoparticles, mainly chemical routes have been followed, such as hydrothermal method, hydrolysis, sol–gel, or coprecipitation methods [3, 36, 37]. For the fabrication of elongated structures and more complex morphologies, synthesis techniques such as electrospinning, thermal oxidation, spray pyrolysis or chemical vapor deposition techniques are commonly employed [38, 39]. Moreover, in order to achieve environmental clean, safe and affordable synthesis methods, green chemistry synthesis of NiO is recently gaining great attention [40].

Some examples of low dimensional NiO structures fabricated following different synthesis routes are shown in Figure 1. NiO nanoparticles with dimensions between 8 and 22 nm synthesized by a sol–gel method are shown in the TEM image in Figure 1A [41]. Fabrication of elongated nano- and microstructures are less extended for NiO. Figure 1B shows a TEM image from a NiO nanorod 5 nm width fabricated by a rapid thermal oxidation under a controlled oxygen atmosphere using Au as a catalyst [39]. A submicrometric NiO hollow sphere synthesized by spray pyrolysis followed by a subsequent controlled heat treatment is shown in the TEM image in Figure 1C [42]. Porous nanobelts arrays with flake appearance synthesized by hydrolysis and etching methods are shown in the Scanning Electron Microscope (SEM) image in Figure 1D [43]. SEM image in Figure 1E shows a rose-like NiO microstructure formed by nanoplates synthesized by a solvothermal method combined with a calcination process [44]. Vapor–solid processes have been recently used for the growth of NiO micro- and nanostructures. The NiO microcrystals with a labyrinth appearance shown in Figure 1F were fabricated following a one-step vapor process method at 1200 °C using metallic Ni as precursor and a controlled Ar flow [45]. SEM image in Figure 1G shows a Sn doped NiO surface with grid patterning as well as microwires some microns length grown by a vapor–solid process at 1400 °C assisted by Sn doping [38]. This route allows to obtain new morphologies not previously reported for NiO, avoiding the use of catalysts and therefore reducing the cost of the processes.

Doping with different elements not only affects to the chemical behaviour or surface states [46] but is also a common strategy to tailor the physico-chemical properties of this transition metal oxide and to achieve improved functionalities. In most cases, the controlled doping process aims to improve the electrical conductivity and magnetic response of NiO by modifying the final stoichiometry, however optical properties can be also tailored by controlling the synthesis process and post treatments. Incorporation of dopants with diverse oxidation states in NiO could lead to variations in the concentration of Ni vacancies as well as a tuned Ni^{2+}/Ni^{3+} ratio in order to reach charge neutrality. In addition, the incorporation of impurity levels in the bandgap can also lead to variable luminescence and tuned optical performance. Diverse elements of technological interest, such as Li, Cu, Sn, Co, Al, and K, among others, have been used as dopants in

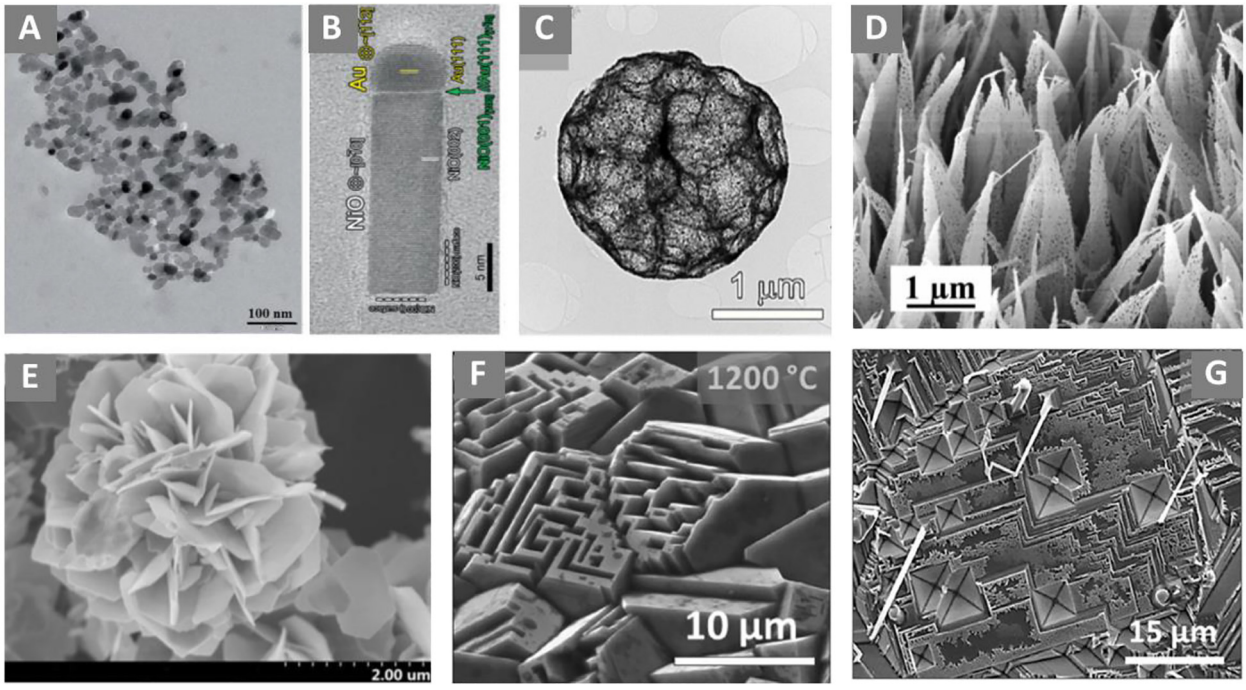

Figure 1: (A) NiO nanoparticles synthesized by sol–gel reproduced from Ref. [41] with permission from the Royal Society of Chemistry. (B) NiO nanorod fabricated by thermal oxidation using Au as a catalyst reproduced from Ref. [39], (C) NiO hollow sphere synthesized by spray pyrolysis reprinted with permission from Ref. [42] Copyright 2018 American Chemical Society. (D) NiO nanobelts synthesized by hydrolysis reproduced with permission from [43]. Copyright (2015) Wiley. (E) Flower-like NiO synthesized by a solvothermal route reprinted from Ref. [44] Copyright 2015, with permission from Elsevier. (F) Labyrinth-like NiO microcrystals fabricated by a vapor-solid process reprinted with permission from Ref. [45] Copyright 2020 American Chemical Society. (G) Sn doped NiO grid-patterning and microwires grown by a vapor-solid method reprinted from Ref. [38] Copyright 2020, with permission from Elsevier.

NiO as a function of the required improved performance [38, 47–50].

3 Optical and optoelectronic applications based on NiO

In this section, emerging NiO-based optical and optoelectronic applications will be reviewed, with special attention paid to the recent developments of lighting devices, optical microresonators, waveguides, optical limiters and neuromorphic devices based on NiO micro- and nanostructures.

3.1 Lighting devices

As a wide bandgap material, NiO can exhibit broad luminescence from the near infrared to the ultraviolet range based on the different recombination levels in the bandgap. The study of the NiO luminescence allows achieving deeper comprehension of the formation of defects during the synthesis, doping and post treatment of the NiO samples, leading as well to improved performance in diverse optical applications. Despite the potential interest of the NiO luminescence, not many works reported on the luminescence of this material so far. To date, mainly photoluminescence (PL) studies have been developed, together with a few studies based on the cathodoluminescence (CL) and electroluminescence (EL). Luminescence from NiO is commonly associated with Ni deficiency, d–d transitions and defect or impurity levels in the bandgap. However, diverse luminescence information can be achieved as a function of the selected luminescence technique.

The optical properties, and therefore the electronic band structure of NiO can be modulated by the size or the presence of dopants in this metal transition oxide [51]. Manikandan et al. [52], reported that for stoichiometric NiO synthesized using a microwave combusting method, only emissions in the UV region (346 nm) can be observed, which should correspond to a near band-edge emission due to the recombination of excitons. This fact confirms that the presence of defects in NiO promoted by several factors, plays a key role in the luminescence properties and therefore in the optical applications of this oxide. Thermodynamically, it is found that nickel vacancies are the most dominant point defects present in NiO, therefore the optical properties of this oxide should be dominated by the radiative emissions promoted for the presence of Ni vacancies. However, the presence of other defects such as oxygen vacancies or interstitials can be also promoted by controlling the experimental conditions.

As some examples related to the luminescent properties of NiO, Figure 2A shows the PL spectra from NiO nanoparticles synthesized by a sol–gel method acquired using a UV laser of 266 nm (4.66 eV) as excitation source [36]. According to the authors, in this case, the luminescence of the NiO nanoparticles is dominated by a deep-level green emission around 520 nm (2.38 eV) together with a weak near band edge emission in the UV range at 333–357 nm (3.47–3.72 eV). Structural defects, such as oxygen/nickel vacancies and interstitials are related with the green emission, while the UV emission is due to excitonic recombinations corresponding to near band-edge transitions in NiO. A scheme showing the different emissions and the related electronic transitions is also depicted in Figure 2B, together with the dependence of the UV emission (Figure 2C) and the band gap energy (Figure 2D) as a function of the crystallite dimensions. In addition to the UV and green emissions previously described, additional contributions can be observed after the deconvolution of the PL spectra. The violet emission at 2.97 eV appeared through the possible transition of trapped electrons at Ni interstitial to the valence band. The blue luminescence peak at 2.70 eV is associated to radiative recombination of electrons from the doubly ionized Ni vacancies to the holes in the valence band. Taking this into account, the structure of defects in NiO can be modified by the selected synthesis route and post-treatments, as well as by doping, leading to variable luminescence, as reported by different authors [48]. Some works report on the PL signal from NiO nanomaterial using lasers with different wavelengths, however, less has been done so far in the study of the CL signal, a technique which can shed light to the deeper comprehension of the levels in the bandgap. Recently, Taeño et al. [45] reported a complete CL study of NiO samples as a function of the sintering temperature. In that study, diverse NiO microstructures were fabricated at temperatures between 800 and 1500 °C under a controlled Ar flow using metallic Ni as precursor material. Figure 2E shows the variable CL emissions acquired at 110 K from the NiO samples as a function of the sintering temperature. This CL signal covers a broad range of energy from the near IR (1.49 eV), to the visible (1.96, 2.22, and 2.55 eV), and the UV (4.43 eV). Both the intensity and the shape of this signal can be tailored as a function of the defects promoted or quenched during the thermal annealing. The complex emission in the visible range 2–2.5 eV is mainly associated with the presence of nickel vacancies, confirmed by the presence of Ni^{3+}, while the near-IR emission is due to transitions involving 3*d* energy levels. High energy emissions in the CL spectrum

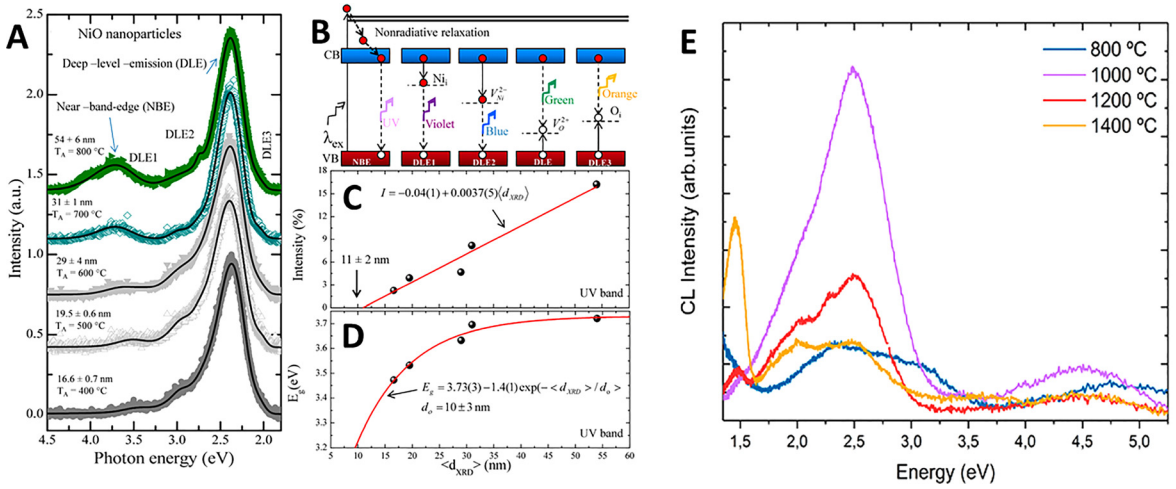

Figure 2: (A) Photoluminescence (PL) spectra from NiO showing dependence with the crystallite size. (B) Proposed electronic transitions between defect levels and bandgap of NiO nanoparticles. (C) Intensity of the UV emission and (D) bandgap energy as a function of the nanoparticles size, reproduced from Ref. [36]. (E) CL spectra acquired at 110 K from NiO samples sintered at 800, 1000, 1200 and 1400 °C. Reprinted with permission from Ref. [45] Copyright 2020 American Chemical Society.

are related to d–d charge transfer excitons in NiO and near band edge emissions. Luminescence from NiO can be also tuned by appropriate doping, however in order to face potential functionalization in luminescent devices the inherent low luminescent intensity from NiO should be overcome. In a recent work, Taeño et al. [38] reported an increase of the luminescence signal from NiO by Sn doping. In this case, the CL signal from Sn doped NiO samples fabricated by thermal treatments at 1400 °C can be increased in a factor ×40 by low Sn doping. In that work, different Sn-based precursors in a variable concentration were used for the achievement of the Sn doped NiO nano- and microstructures in forms of grid-self assembled complex surfaces and microwires. The luminescence of these NiO microstructures covers a wide range of energies, with emissions in the near-IR (1.46 eV), the visible (2–2.5 eV) and the UV range (3.5 and 4.5 eV), the relative intensity of which can be tuned as a function of the composition of the precursor mixture, as shown in Figure 3A. Appropriate Sn doping can also tune the NiO luminescence from the near-IR to the UV. The chromaticity diagram obtained from the CL spectra in Figure 3A is shown in Figure 3B.

Similarly to other metal oxides, modulation of the NiO luminescence can be achieved by controlling the synthesis method, the doping process as well as by treatments under diverse atmospheres. Hence, either monochromatic or wide luminescence can be obtained as a function of the requirements for the NiO based luminescent device. The

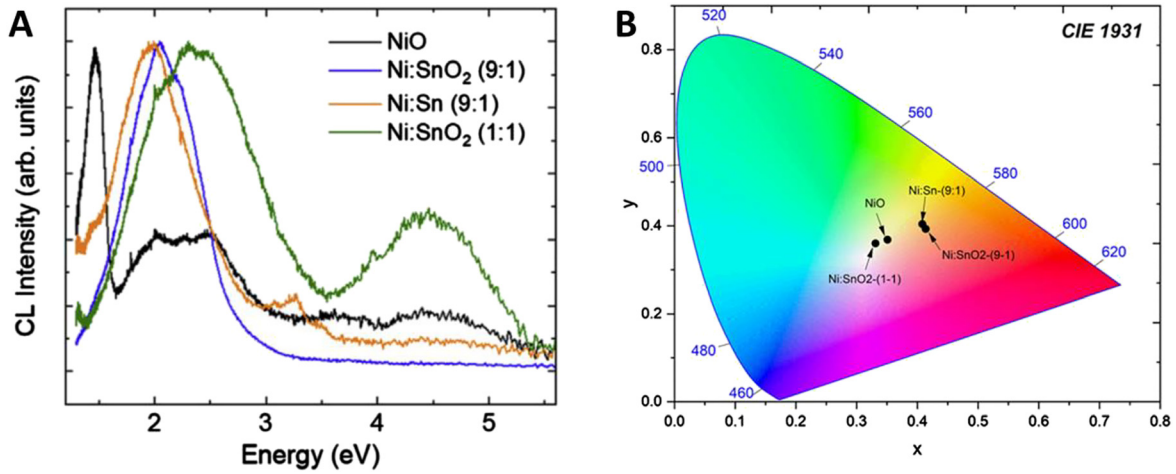

Figure 3: (A) Normalized cathodoluminescence (CL) spectra from NiO and Sn doped NiO samples grown at 1400 °C using different precursors and (B) CIE 1931 chromaticity coordinates from spectra in (A). Reprinted from Ref. [38] Copyright 2020, with permission from Elsevier.

capability of emitting broadband white light also reveals promising applicability of NiO in white-light emitters without the need of phosphors or quantum well structures.

Based on the excellent optoelectronic properties of NiO, it has been also considered as a great candidate in light-emitting-diodes (LEDs), as a constituent of a *p*–*n* heterojunction, and more recently in quantum-dot LEDs (Q-LEDs) and organic–inorganic hybrid LEDs (Hy-LEDs). The characteristic high work function and large ionization energy of this *p*-type oxide, as well as its good stability and carrier transport performance, make it an excellent candidate to be exploited in solid state lighting devices, as demonstrated in recent scientific works. It should be noted that the achievement of reliable *p*-type doping in most semiconducting oxides such as Ga_2O_3, ZnO, SnO_2, In_2O_3, and TiO_2 is a difficult and controversial task which hinders the development of homojunction LEDs and other optical devices. Therefore, an alternative strategy is to fabricate *p*–*n* heterojunctions by integrating *n*-type and *p*-type semiconducting oxides if the interface quality is controlled in a proper manner. Among the *p*-type oxides, NiO arouses increased interest due to its optimal electro-optical properties and stability, which motivates its use in heterojunction LEDs based in oxide materials. As some examples, Xi et al. [53] reported on the fabrication of a *p*-type NiO/*n*-type ZnO based LED using low temperature solution-based growth methods. In that case, the initial negligible light emission from the as-grown NiO film was improved by annealing. The electroluminescence signal depends on the bias voltage, leading to intense UV emission for high bias voltages. Figure 4A shows the *I*–*V* curves of different devices based on the NiO/ZnO system with variable layers, where a diode-like behavior can be observed for all the devices. Despite the low efficiency exhibited by these devices (maximum emission power 0.14 μW/cm^2 at 23 V bias) it could be easily improved by optimized design, tuning of the oxides properties, and insertion of organic layers. In recent years, Q-LEDs have attracted increasing interest as these devices demonstrated high fluorescence efficiency, long fluorescence life, and large luminosity. Furthermore, Q-LEDs can exhibit adjustable emission spectrum as a function of the bandgap width of the quantum dots (QD). Indeed, Q-LEDs are expected to be one of the most promising candidates in the next generation lighting devices. The singular optoelectronic properties of NiO make it useful for hole transport and electronic barrier material in these devices. In order to overcome some of the electronic drawbacks which could hinder the applicability of NiO, doping with different elements was employed to improve its hole mobility and conductivity, thus leading to enhanced current efficiency. Zhang et al. [37] reported the synthesis of Fe doped NiO nanocrystals by a solvothermal route used as a hole injector layer in a Q-LED with competitive results. Enhanced fluorescence intensity was achieved in this case by increasing Fe doping, mainly due to passivation of the surface defect states of NiO and a decrease of the exciton quenching effect on the quantum dot light emitting layer. Figure 4B shows the current efficiency as a function of the luminance for different Fe doping in the Fe doped NiO based Q-LEDs. By 5 mol% Fe doping in NiO, enhanced carrier concentration and electrical conductivity were achieved. Maximum values of luminescence, quantum efficiency (3.84%) and current efficiency (5.93 cd/A) were achieved for the Q-LED showing long lifetime of 11,490 h. Inset in Figure 4B shows the excellent monochromacity of one red QLED based on Fe doped NiO at an applied voltage of 5 V.

NiO has been also used as hole injection layer in organic–inorganic hybrid LEDs (Hy-LEDs). The low cost, scalability and mechanical properties of these hybrid LED make them interesting candidates in solid state lighting devices and flexible-display technologies [47, 54]. In a

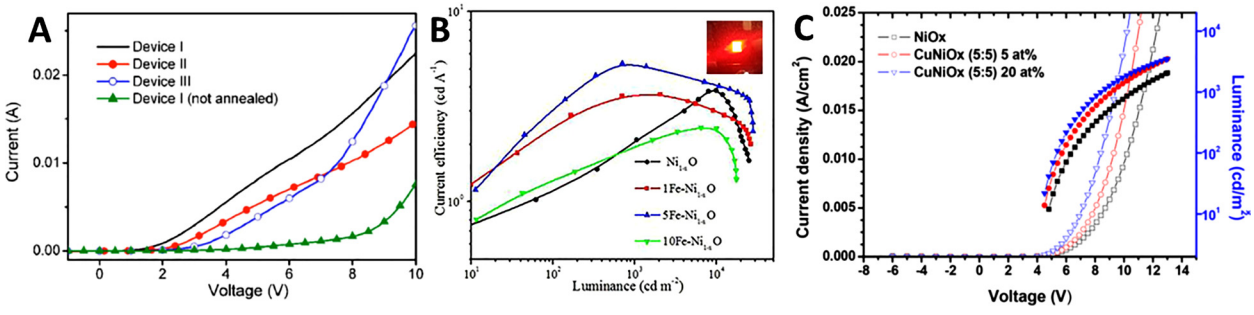

Figure 4: (A) *I*–*V* curves from the different heterojunction devices, reprinted from [53] with permission of AIP publishing. (B) Current efficiency versus luminance of the Q-LEDs. The inset in (B) shows a digital photograph of the c-based Q-LED under a 5 V applied voltage. Reprinted from Ref. [37] Copyright 2020, with permission from Elsevier. (C) Current density–voltage–luminance curves of the hybrid LEDs (Hy-LEDs) – reprinted with permission from Ref. [47] Copyright 2018 American Chemical Society.

recent work, Kim et al. [47] reported on the use of Cu (I) and Cu (II) codoped NiO films synthesized by sol–gel which exhibit high ionization energy, as well as improved conductivity and hole injection ability due to the large amount of Ni vacancies promoted by Cu co-doping. In that case, an improved performance was achieved for the Cu codoped NiO films, as compared with pristine NiO. Figure 4C shows the current density–voltage–luminance curves both from pristine NiO_x and Cu codoped NiO based devices. It can be clearly observed that both the current density and the luminance increase for the Cu codoped NiO based devices, based on an enhancement of the hole density in the emitting layer. Moreover, the NiO-based hole injection layer induces a well-balanced electron and hole charge injection. A current efficiency of 15.4 cd/A at 500 cd/m^2 was achieved for the Hy-LED with 5 at.% Cu codoped NiO_x, which in this case shows a maximum of the electroluminescence signal in the green range (510 nm).

As previously mentioned, NiO has been also employed as a constituent in *p*–*n* heterojunctions diodes. Recently, Gong et al. [55] constructed NiO/β-Ga_2O_3 *p*–*n* heterojunctions diodes by a double layer design of NiO with varied hole concentrations. According to the authors, by reducing the hole concentration from 3.6×10^{19} to 5.1×10^{17} cm^{-3}, the leakage current density is reduced to 10^{-9} A/cm^2 while a high rectification ratio over 10^{10} is still maintained even operating at high temperature of 400 K. The results showed that the resultant device possesses a record high breakdown voltage (V_b) of 1.86 kV compared with other β-Ga_2O_3 based *p*–*n* heterojunction diodes [56]. The improvement breakdown voltage is attributed to the suppression of electric field crowding by decreasing hole concentration in NiO.

3.2 Optical resonators and waveguides

The applicability of NiO as building blocks in some optical devices requires the fabrication of low dimensional structures with improved optical properties and well-defined dimensions and morphology, which in some cases involves the upgrade of the synthesis methods. Over the last years, the development of low dimensional optical microcavities has aroused great attention as they can be used in devices in which light confinement is required, such as lasers, optical resonators, filters, and waveguides, among others. In this frame, some authors reported on the use of different semiconducting oxides microstructures with variable morphologies in form of microtubes and microrods with hexagonal or rectangular cross-sections, as low dimensional optical resonators in which Fabry–Perot (FP) resonances due to light reflections between the opposed flat ends of the cavity and/or whispering gallery modes (WGM) involving total internal reflections around the inner faces of the cavity can occur [57–59]. However, despite the potential applicability of NiO in these types of optical devices, it has been only recently that NiO-based resonant cavity modes have been reported [60, 61]. In that work, FP modes were observed in the visible range and analyzed for NiO microcrystals with lateral dimensions around 10 μm fabricated by thermal treatments at 1200 °C (Figure 5A). Light confinement and optical resonances are favoured by the singular geometry, flat and well-faceted surfaces and high crystalline quality of the as-grown NiO microstructures. Among the probed microcrystals, only those with smooth surfaces exhibit clear modulations in the corresponding photoluminescence spectrum acquired with an UV laser (λ = 325 nm), as shown in Figure 5B which

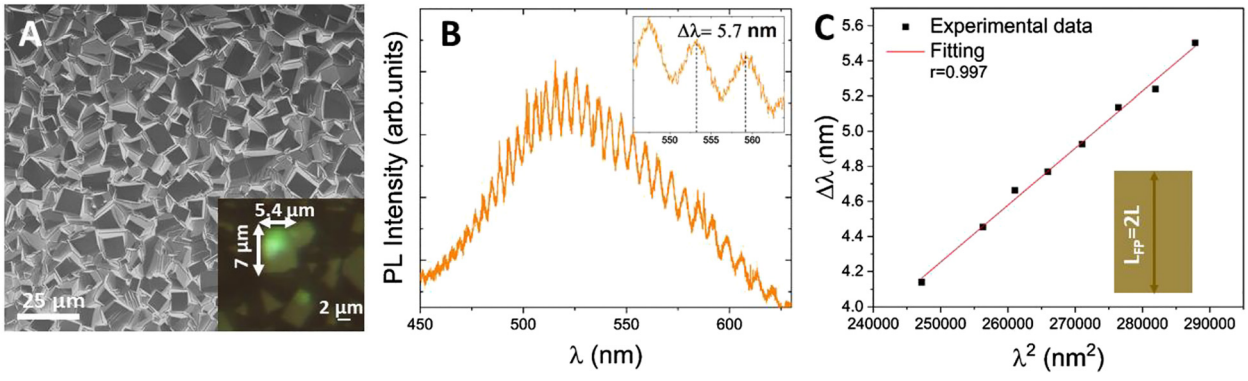

Figure 5: (A) Scanning Electron Microscope (SEM) image from NiO microcrystals. Inset in (A) shows an optical image from a detailed region with NiO microcrystals. (B) Photoluminescence (PL) spectrum from the microcrystal in the inset in (A) showing optical modulations, enlarged in the inset. (C) $\Delta\lambda$ versus λ^2 from the analysis of the PL signal in (B) with the corresponding linear fitting. Reprinted from Ref. [60] Copyright 2021, with permission from Elsevier.

corresponds to the microcrystal shown in the optical image included as an inset in Figure 5A. A detailed analysis of the modulated signal and the mode spacing, included in Figure 5C, indicated that the NiO microcrystals behave as Fabry–Perot optical microcavities, although the presence of WGM cannot be disregarded. An experimental refractive index of $n = 2.3 \pm 0.2$ was also obtained from the analysis of the resonances observed in the NiO microcrystals. Besides, quality (Q) and finesse (F) factors around 207 and 1.8, respectively, were calculated for the microcavities, which can be further improved by an exhaustive control of the morphology and dimensions of these NiO microstructures. Moreover, a method for the fabrication of a platform with multiple NiO based optical resonators is proposed, avoiding complex post treatments or single structures manipulation [61].

As previously mentioned, the fabrication of NiO elongated microstructures has not been deeply explored so far. However, based on preliminary works, NiO elongated structures with different morphology and dimensions can be obtained as a function of the experimental conditions and Sn-based precursor. As an example, Figure 6A shows a SEM image of Sn doped NiO microwires obtained following a vapor–solid method at 1400 °C using metallic Ni and SnO_2 as precursors materials. The growth of these microwires is favoured by the presence of Sn-based compounds in the precursor mixture. When using a mixture of metallic Ni and SnO_2, the as-grown microwires show smooth surfaces and regular cross sections, with lengths of tens of μm and widths of a few microns, as shown in Figure 6A. The singular geometry and dimensions of these NiO microwires could favour their applicability as building block in optical devices. Moreover, these microwires exhibit waveguiding behaviour, as the light from a He–Ne red laser (633 nm) can be guided along the microstructure without large losses, which can wide the optical applicability of NiO. It should be noted that this behaviour has not been previously reported for NiO, to the best of our knowledge. Figure 6B shows an optical image from the Sn doped NiO microwires deposited onto a silicon substrate while Figure 6C shows the bright field optical image in which a waveguiding behaviour can be observed in the marked microwire. When the microwire is illuminated by one end a bright signal light can be observed in the opposite end, thus confirming the waveguiding behavior.

3.3 Optical limiters and biomedical applications

Among the emerging optical functionalities based on the multifunctional photonic properties of NiO, recent advances have been reported on its use as optical limiter, saturable absorber and optical switch. Over the last years, optical limiting devices exhibited large applicability as optical switches, mode lockers, and optical safety. Actually, in order to avoid potential damage under intense laser condition, the use of appropriate optical limiters is mandatory in photonic sensors, including the human eye as well. Furthermore, the passive saturable absorbers exhibit advantages in the fabrication of Q-switching and mode-locking pulses, as compared with other active techniques, mainly due to the low cost and easy fabrication of the formers.

The inherent optical properties of NiO, such as the suitable wide bandgap and low saturation intensity, make this material a promising saturable absorber mainly around the 2 μm spectral region. It should be noted that the use of fiber lasers operating in the midinfrared spectral region (~2 μm) is required in applications including telecommunications, medical surgery, and light detection and ranging. Besides, many advantages can be achieved in this spectral range as falls into the “eye-safe laser” category [62]. As an example, thulium and holmium based active

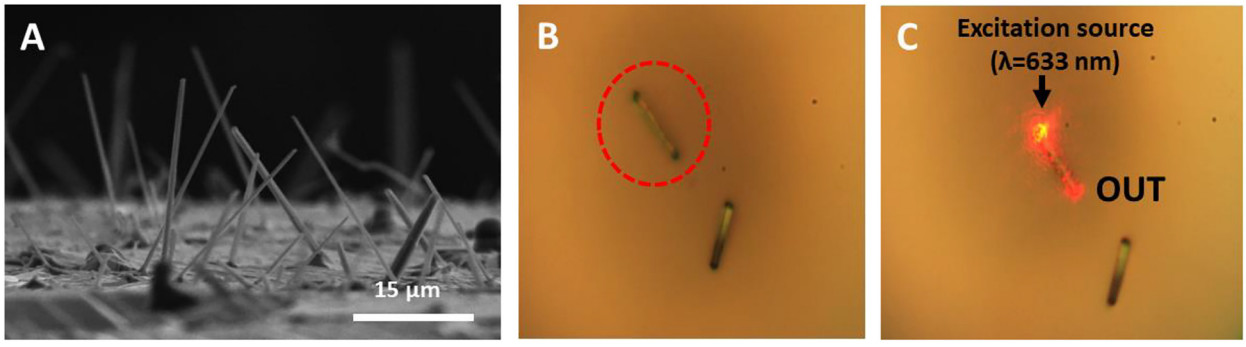

Figure 6: (A) Scanning Electron Microscope (SEM) image from NiO microwires fabricated using Ni and SnO_2 in the starting mixture. (B) Optical images from the NiO microwires placed onto a Si substrate and (C) bright field image from Ni:SnO_2 microwire showing waveguiding behaviour under a red laser illumination.

fibers are suitable for ultrashort pulses generation and to fabricate lasers with wideband wavelength tuning. Recently, Rusdi et al. [63] reported the fabrication of Q-switching and mode-locked fiber lasers operating in the spectral range ~2 μm using a saturable absorber film based on NiO nanoparticles synthesized by a sonochemical method. The proposed set up for the thulium doped fiber laser is shown in Figure 7A. Figure 7B shows the output spectrum of the laser, at the corresponding threshold powers, operating at different regimes: continues wave (CW), Q-switching and mode-locking modes, as well as enlarge details of each individual spectrum. It can be observed how the CW laser transits into Q-switched by inserting the NiO saturable absorber. Without NiO in the cavity, the CW laser is stablished centered at 1955.60 nm (Figure 7C). When the pump power raises, the CW laser transits into Q-switched peaked at 1928.82 nm, which shows a broader profile (Figure 7D). At higher pump power, selfgenerated mode-locked centered at 1900.52 nm can be observed (Figure 7E). It should be noted that as the pump power is raised the number of laser modes increases as well. As a result of the insertion of the NiO saturable absorber, a laser peak shifting is also observed, due to the changes in the cavity loss.

Besides, further improvements in the design of optical devices could be achieved by the controlled electron transition processes and the corresponding tuned optical properties of NiO. As a recent example, Sun et al. [64] reported the use of NiO nanosheets as saturable absorber in ultrafast lasers. The authors synthesized NiO nanosheets with dimensions around 150–200 nm following a hydrothermal method and describe their optical behaviour which can be tailored as a function of the thickness of the nanosheets, leading to saturable and reverse saturable absorption, as a function of the intra-band transitions balanced processes. In this case, NiO nanosheets with optimized thickness have been employed as a broad optical modulator based on their saturable absorption effect. Diode-pumped broadband mode-locked lasers with wavelengths of 1.06 and 1.34 μm were developed based on a NiO sample optimized for saturable absorption, as schemed in Figure 8A. Figures 8B shows the mode-locked pulse with a Gaussian profile, while the spectrum in Figure 8C shows the output spectrum centered at 1.06 μm

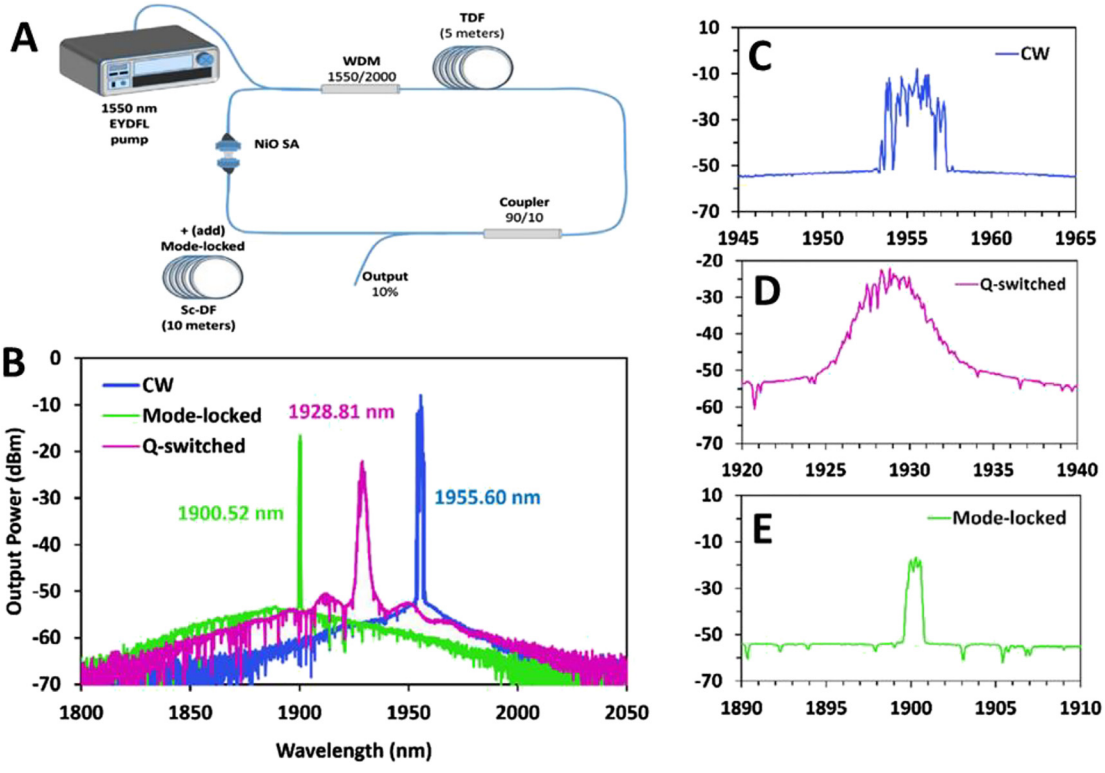

Figure 7: (A) Scheme of the thulium doped fiber laser. (B) Output spectra of the continues wave (CW), Q-switched and mode locked fiber laser at the respective threshold pump powers. Each detailed spectrum is shown in (C), (D), and (E). Reprinted from Ref. [63] Copyright 2019, with permission from Elsevier.

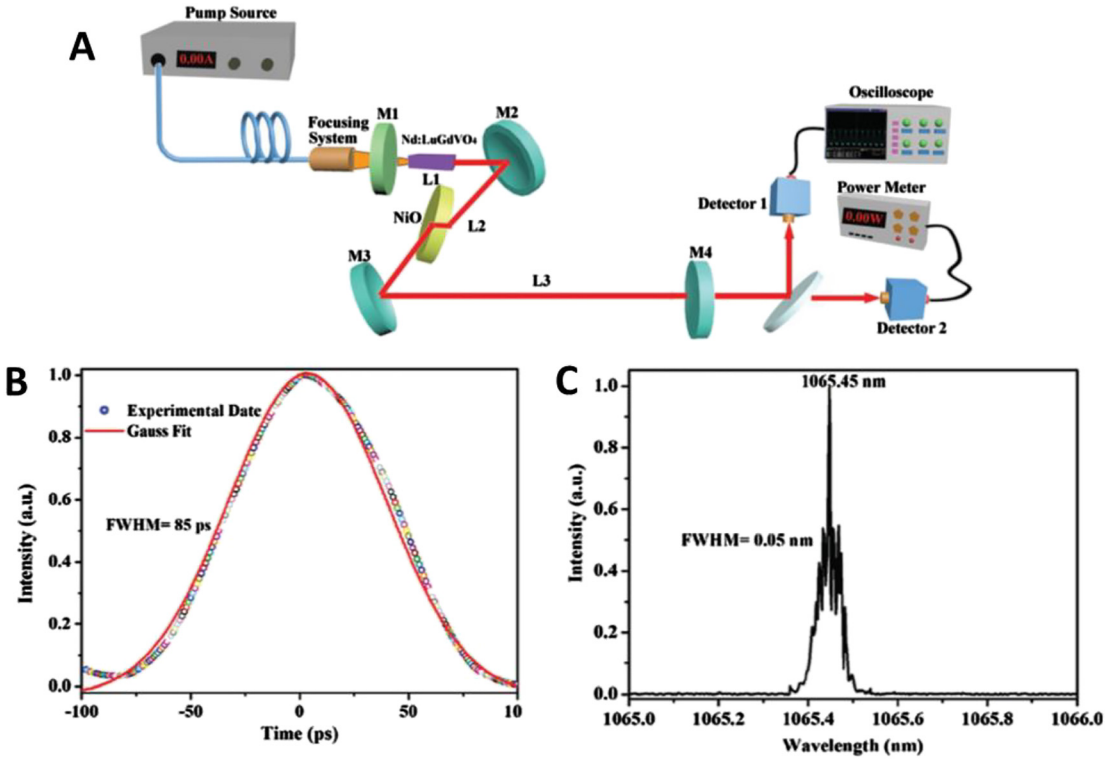

Figure 8: (A) Experimental configuration of diode pumped mode-locked laser using NiO as saturable absorber. (B) Single pulse and (C) output spectrum centered at 1.06 μm from a mode-locked laser using NiO nanosheets as saturable absorber. Reproduced with permission from [64], Copyright (2017) Wiley.

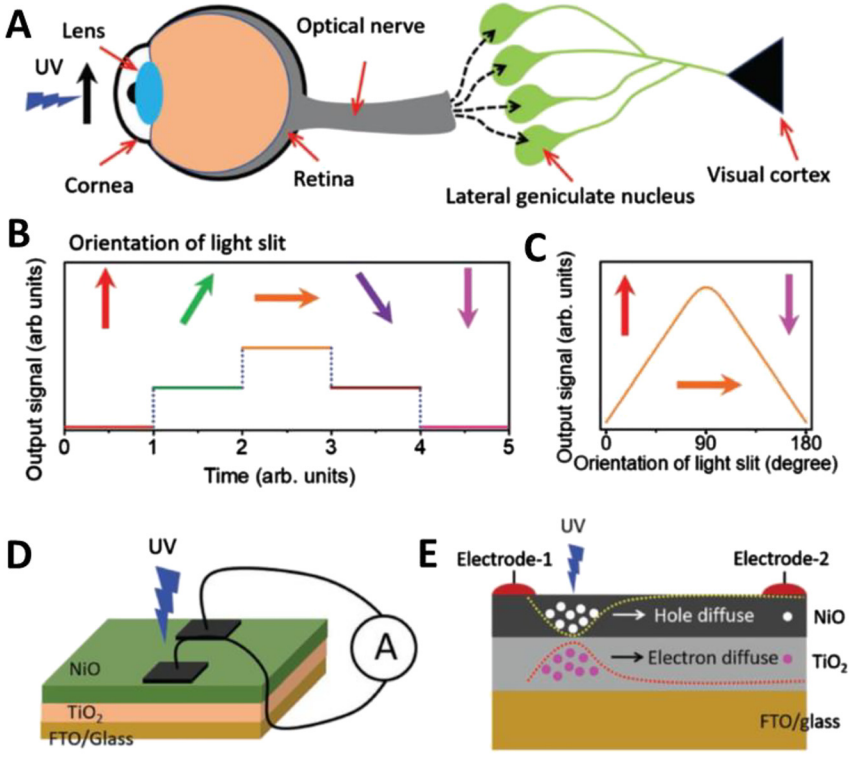

Figure 9: (A) Scheme of the operation of the human eye. (B) Variation in the output response of the visual cortex as a function of the light orientation and (C) Light orientation-dependent response. (D) Proposed NiO/TiO_2 heterostructure with two planar contacts under UV illumination. (E) Lateral photocurrent due to the generation of *e*–*h* pairs by illumination near electrode 1 and charge carriers diffusion towards electrode 2. Reproduced with permission from [65] Copyright (2019) Wiley.

with a full-width half-maximum of 0.05 nm at the central wavelength.

As a proof of the versatility of NiO, this material is earning a place among biomedical optics, as recently reported by Kumar et al. [65] which developed a NiO-based optical device that mimics the primitive functions of the visual cortex. At the forefront of the neuromorphic applications, including artificial visual processing, the development of optoelectronic devices emulating the visual cortex using optical stimuli under self-biased conditions will play key role in future biomedical optical applications. Among other requirements, these neuromorphic devices should accomplish low processing energy, for which photonic triggered devices operating in self-biased conditions, as those described by Kumar et al., appear as promising candidates. In this work [65], the authors developed a high transparent all oxide NiO/TiO_2-based optoelectronic device with brain-like functionalities which mimics the operation and response of the visual cortex. The NiO films 30 nm thick were grown as a part of the NiO/TiO_2 heterostructure using a reactive sputtering with a Ni target (99.999% purity). As stated by the authors, the final micrometric dimensions of the device could be further reduced by future advanced photolithography processes. The operation of the device is based on the generation of a lateral photovoltaic current under nonuniform illumination. The input illuminating photons should induce electron-hole pairs in the heterostructure and lead to a photocurrent collected by two top planar Ag contacts. As the photocurrent outputs correlate with the spatially distributed optical inputs, the device exhibits orientation selective response, which is essential in the achievement of the neuromorphic artificial vision.

The selection of NiO as an active component of this device is not only based on its inherent *p*-type conductivity, but also on its characteristic wide bandgap, which allows high transmittance in the visible range, and its work-function which in combination with TiO_2 leads to the formation of a separation charge layer leading to the separation of the photogenerated hole-electron pairs and preventing their recombination.

Figure 9A shows a scheme of the human eye operation where the optical information is transferred to the visual cortex via the optic nerve. The sensitivity to the light orientation and the orientation dependent response of the visual cortex are shown in Figure 9B and C, respectively. The proposed NiO/TiO_2 based device is schemed in Figure 9D, where two planar contacts collect the current when the UV illumination reaches the surface. The photoinduced holes, in NiO, and electrons, in TiO_2, diffuse laterally from the illuminated electrode 1 to electrode 2, marked in Figure 9E, leading to the generation of lateral photocurrent. In addition to lateral photovoltaic generation and photoresponse dependent on the orientation, this device also exhibits switching behaviour with rise and fall times of 3 and 6 ms, respectively. This self-biased device with orientation dependent response could pave the way to the development of artificial visual systems.

4 Conclusions

To summarize, recent progress on emerging optical and optoelectronic devices based on NiO are reviewed in this work. This transition metal oxide is one of the very few *p*-type oxide, which interesting physico-chemical properties provide wide applicability in diverse fields of technological research. However, less has been done so far in the development of NiO-based optical and optoelectronic devices, despite the potential use of this oxide in the optical field. To date, apart from the well-known use of this material in electrochromic devices and smart windows, where NiO is of prime choice, as well as a hole injector layer in emerging photovoltaic devices, less has been done so far in the development of NiO based optical devices. The quest for innovative optical devices requires the use of materials which accomplish novel applicability and improved performance. In this regard, over the last years a growing number of high impact research works points out to the potential use of NiO in diverse optical and optoelectronic applications, leading to a young and promising research line in which there is still room for improvement. The present review comprises an overview of emerging optical and optoelectronics applications based on NiO micro- and nanostructures. Either undoped and doped NiO nanomaterial synthesized by diverse synthesis routes are included in this work. Firstly, the use of NiO in lighting devices, including Q-LEDs and Hy-LEDS, is reviewed, with special attention paid to the presence of defects and impurity levels in the bandgap and to the enhancement of the luminescence intensity. Secondly, NiO microstructures in form of microcrystals and microwires fabricated by a vapor–solid process are reviewed based on their demonstrated use as optical resonators and waveguides. Fabry–Perot modes have been recently described and analyzed in NiO microcrystals. The achievement of these microstructures with controlled and well-defined morphology allows their use in optical devices. Thirdly, the use of NiO as saturable absorber in optical limiter devices and ultrafast lasers is also described, mainly in the range of ~2 μm. Finally, biomedical optical applications such as a neuromorphic device which mimics the operation and response

of the virtual cortex is reviewed as well, paving the way to the development of neuromorphic artificial vision. These emerging optical and optoelectronic NiO-based applications can open a promising field of research based on this *p*-type material where further improvements are still under development.

Author contributions: All the authors have accepted responsibility for the entire content of this submitted manuscript and approved submission.

Research funding: This work was supported by MINECO/FEDER/M-ERA.Net Cofund projects: MAT 2015-65274-R, RTI2018-097195-B-100 and PCIN-2017-106. This research has received funding from the European Union's Horizon 2020 research and innovation programme under Grant Agreement No. 957225, project BAT4EVER.

Conflict of interest statement: The authors declare no conflicts of interest regarding this article.

References

[1] D. P. Dubal, P. Gómez-Romero, B. R. Sankapal, and R. Holze, "Nickel cobaltite as an emerging material for supercapacitors: an overview," *Nano Energy*, vol. 11, pp. 377–399, 2015.

[2] Y. Chen, O. Sakata, R. Yamauchi, et al., "Lattice distortion and electronic structure of magnesium-doped nickel oxide epitaxial thin films," *Phys. Rev. B*, vol. 95, p. 245301, 2017.

[3] M. Bonomo, "Synthesis and characterization of NiO nanostructures: a review," *J. Nanoparticle Res.*, vol. 20, no. 8, p. 222, 2018.

[4] K. S. Usha, R. Sivakumar, and C. Sanjeeviraja, "Optical constants and dispersion energy parameters of NiO thin films prepared by radio frequency magnetron sputtering technique," *J. Appl. Phys.*, vol. 114, p. 123501, 2013.

[5] C. Park, J. Kim, K. Lee, S. K. Oh, H. Kang, and N. Park, "Electronic, optical, and electrical properties of nickel oxide thin films grown by RF magnetron sputtering," *Appl. Sci. Converg. Technol.*, vol. 24, pp. 72–76, 2015.

[6] M. Napari, T. N. Huq, T. Maity, et al., "Antiferromagnetism and *p*-type conductivity of nonstoichiometric nickel oxide thin films," *InfoMat*, vol. 2, pp. 769–774, 2020.

[7] C. C. Diao, C. Y. Huang, F. Yang, and C. C. Wu, "Morphological, optical, and electrical properties of *p*-type nickel oxide thin films by nonvacuum deposition," *Nanomaterials*, vol. 10, no. 4, p. 636, 2020.

[8] Z. Wang, H. Zhou, D. Han, and F. Gu, "Electron compensation in *p*-type 3DOM NiO by Sn doping for enhanced formaldehyde sensing performance," *J. Mater. Chem. C.*, vol. 5, pp. 3254–3263, 2017.

[9] A. Mallikarjuna Reddy, A. Sivasankar Reddy, K. S. Lee, and P. Shreedhara Reddy, "Effect of oxygen partial pressure on the structural, optical and electrical properties of sputtered NiO films," *Ceram. Int.*, vol. 37, no. 7, pp. 2837–2843, 2011.

[10] A. N. Banerjee, C. K. Ghosh, and K. K. Chattopadhyay, "Effect of excess oxygen on the electrical properties of transparent *p*-type conducting $CuAlO_x^{2+}$ thin films," *Sol. Energy Mater. Sol. Cells*, vol. 89, no. 1, pp. 75–83, 2005.

[11] X. Xu, L. Li, J. Huang, et al., "Engineering Ni^{3+} cations in NiO lattice at the atomic level by Li^+ doping: the roles of Ni^{3+} and oxygen species for CO oxidation," *ACS Catal.*, vol. 8, no. 9, pp. 8033–8045, 2018.

[12] R. Kumar, C. Baratto, G. Faglia, G. Sberveglieri, E. Bontempi, and L. Borgese, "Tailoring the textured surface of porous nanostructured NiO thin films for the detection of pollutant gases," *Thin Solid Films*, vol. 583, pp. 233–238, 2015.

[13] Y. Ku, C-N. Lin, and W-M. Hou, "Characterization of coupled NiO/TiO_2 photocatalyst for the photocatalytic reduction of Cr(VI) in aqueous solution," *J. Mol. Catal. Chem.*, vol. 349, no. 1, pp. 20–27, 2011.

[14] G. Cai, X. Wang, M. Cui, et al., "Electrochromo-supercapacitor based on direct growth of NiO nanoparticles," *Nanomater. Energy*, vol. 12, pp. 258–267, 2015.

[15] D. U. Lee, J. Fu, M. G. Park, H. Liu, A. Ghorbani Kashkooli, and Z. Chen, "Self-assembled NiO/$Ni(OH)_2$ nanoflakes as active material for high-power and high-energy hybrid rechargeable battery," *Nano Lett.*, vol. 16, no. 3, pp. 1794–1802, 2016.

[16] F. Shahzad, K. Nadeem, J. Weber, H. Krenn, and P. Knoll, "Magnetic behavior of NiO nanoparticles determined by SQUID magnetometry," *Mater. Res. Express*, vol. 4, no. 8, 2017, https://doi.org/10.1088/2053-1591/aa8674.

[17] A. Dewan, S. Haldar, and R. Narayanan, "Multi-shelled NiO hollow microspheres as bifunctional materials for electrochromic smart window and non-enzymatic glucose sensor," *J. Solid State Electrochem.*, vol. 25, pp. 821–830, 2021.

[18] S. Jin, S. Wen, M. Li, H. Zhong, Y. Chen, and H. Wang, "Effect of the grain size on the electrochromic properties of NiO films," *Opt. Mater.*, vol. 109, p. 110280, 2020.

[19] L. Hu, J. Peng, W. Wang, et al., "Sequential deposition of CH3NH3PbI3 on planar NiO film for efficient planar perovskite solar cells," *ACS Photonics*, vol. 1, no. 7, pp. 547–553, 2014.

[20] W. Chen, Y. Wu, J. Fan, et al., "Understanding the doping effect on NiO: toward high-performance inverted perovskite solar cells," *Adv. Energy Mater.*, vol. 8, no. 19, pp. 1–10, 2018.

[21] P. Qin, M. Linder, T. Brinck, G. Boschloo, A. Hagfeldt, and L. Sun, "High incident photon-to-current conversion efficiency of *p*-type dye-sensitized solar cells based on NiO and organic chromophores," *Adv. Mater.*, vol. 21, no. 29, pp. 2993–2996, 2009.

[22] A. Nattestad, A. Mozer, M. K. Fischer, et al., "Highly efficient photocathodes for dye-sensitized tandem solar cells," *Nat. Mater.*, vol. 9, pp. 31–35, 2009.

[23] H. Hakkoum, T. Tibermacine, N. Sengouga, et al., "Effect of the source solution quantity on optical characteristics of ZnO and NiO thin films grown by spray pyrolysis for the design NiO/ZnO photodetectors," *Opt. Mater.*, vol. 108, p. 110434, 2020.

[24] H. K. Li, T. P. Chen, S. G. Hu, et al., "Highly spectrum-selective ultraviolet photodetector based on *p*-NiO/*n*-IGZO thin film heterojunction structure," *Opt. Express*, vol. 23, no. 21, p. 27683, 2015.

[25] K. Kakiage, Y. Aoyama, T. Yano, K. Oya, J. Fujisawa, and M. Hanaya, "Highly-efficient dye-sensitized solar cells with

collaborative sensitization by silyl-anchor and carboxy-anchor dyes," *Chem. Commun.*, vol. 51, pp. 15894–15897, 2015.
[26] I. R. Perera, T. Daeneke, S. Makuta, et al., "Application of the tris(acetylacetonato)iron(III/II) redox couple in *p*-type dye-sensitized solar cells," *Angew. Chem.*, vol. 54, pp. 3758–3762, 2015.
[27] S. K. Kim, H. J. Seok, D. H. Kim, et al., "Comparison of NiO_x thin film deposited by spin-coating or thermal evaporation for application as a hole transport layer of perovskite solar cells," *RSC Adv.*, vol. 10, p. 43847, 2020.
[28] S. Liu, L. Hu, S. Huang, et al., "Enhancing the efficiency and stability of PbS qauntum dot solar cells through engineering and ultrathin NiO nanocrystalline interlayer," *ACS Appl. Mater. Interfaces*, vol. 12, no. 41, pp. 46239–46246, 2020.
[29] S. Chakrabarti, D. Carolan, B. Alessi, P. Maguire, V. Svrcek, and D. Mariotti, "Microplasma-synthesized ultra-small NiO nanocrystals, a ubiquitous hole transport material," *Nanoscale Adv.*, vol. 1, pp. 4915–4925, 2019.
[30] P. Baraskar, R. J. Choudhary, P. K. Sen, and P. Sen, "Dispersive optical nonlinearities and optical path length compensation in NiO/Al doped NiO bilayer thin film," *Opt. Mater.*, vol. 96, p. 109278, 2019.
[31] R. Chouhan, P. Baraskar, A. Agrawal, M. Gupta, P. K. Sen, and P. Sen, "Effects of oxygen partial pressure and annealing on dispersive optical nonlinearity in NiO thin films," *J. Appl. Phys.*, vol. 122, no. 2, p. 025301, 2017.
[32] V. P. Patil, S. Pawar, M. Chougule, et al., "Effect of annealing on structural, morphological, electrical and optical studies of nickel oxide thin films," *JSEMAT*, vol. 1, no. 2, pp. 35–41, 2011.
[33] V. Ganesh, B. Ravi Kumar, Y. Bitla, I. S. Yahia, and S. Alfaify, "Structural, optical and dielectric properties of Nd doped NiO thin films deposited with a spray pyrolysis method," *J. Inorg. Organomet. Polym. Mater.*, 2021. https://doi.org/10.1007/s10904-021-01889-3.
[34] J. R. Abenuz Acuña, S. Perez, V. Sosa, et al., "Sputtering power effects on the electrochromic properties of NiO films," *Optik*, vol. 231, p. 166509, 2021.
[35] P. Salunkhe, A. V. M. Ali, and D. Kekuda, "Investigation on tailoring physical properties of nickel oxide thin films grown by dc magnetron sputtering," *Mater. Res. Express*, vol. 7, p. 016427, 2020.
[36] A. Gandhi and S. Wu, "Strong deep-level-emission photoluminescence in NiO nanoparticles," *Nanomaterials*, vol. 7, no. 8, p. 231, 2017.
[37] Y. Zhang, X. Wang, Y. Chen, and Y. Gao, "Improved electroluminescence performance of quantum dot light-emitting diodes: a promising hole injection layer of Fe-doped NiO nanocrystals," *Opt. Mater.*, vol. 107, p. 110158, 2020.
[38] M. Taeño, D. Maestre, and A. Cremades, "Fabrication and study of self-assembled NiO surface networks assisted by Sn doping," *J. Alloys Compd.*, vol. 827, p. 154172, 2020.
[39] K. Koga, and M. Hirasawa, "Gas-phase generation of noble metal-tipped NiO nanorods by rapid thermal oxidation," *Mater. Res. Express*, vol. 1, no. 4, p. 045021, 2015.
[40] B. Wang, J. S. Chen, Z. Wang, S. Madhavi, and X. W. Lou, "Green synthesis of NiO nanobelts with exceptional pseudo-capacitive properties," *Adv. Energy Mater.*, vol. 2, no. 10, pp. 1188–1192, 2012.
[41] S. Pilban Jahromi, A. Pandikumar, B. T. Goh, et al., "Influence of particle size on performance of a nickel oxide nanoparticle-based supercapacitor," *RSC Adv.*, vol. 5, no. 18, pp. 14010–14019, 2015.
[42] B. Y. Kim, J. W. Yoon, J. K. Kim, Y. C. Kang, and J. H. Lee, "Dual role of multiroom-structured Sn-doped NiO microspheres for ultrasensitive and highly selective detection of xylene," *ACS Appl. Mater. Interfaces*, vol. 10, no. 19, pp. 16605–16612, 2018.
[43] Y. Zhang, W. Zhang, Z. Yang, et al., "Self-sustained cycle of hydrolysis and etching at solution/solid interfaces: a general strategy to prepare metal oxide micro-/nanostructured arrays for high-performance electrodes," *Angew. Chem. Int. Ed.*, vol. 54, no. 13, pp. 3932–3936, 2015.
[44] M. Yao, Z. Hu, Y. Liu, P. Liu, Z. Ai, and O. Rudolf, "3D hierarchical mesoporous roselike NiO nanosheets for high-performance supercapacitor electrodes," *J. Alloys Compd.*, vol. 648, pp. 414–418, 2015.
[45] M. Taeño, J. Bartolomé, L. Gregoratti, P. Modrzynski, D. Maestre, and A. Cremades, "Self-organized NiO microcavity arrays fabricated by thermal treatments," *Cryst. Growth Des.*, vol. 20, no. 6, pp. 4082–4091, 2020.
[46] Z. Xu and J. R. Kitchin, "Relationships between the surface electronic and chemical properties of doped 4*d* and 5*d* late transition metal dioxides," *J. Chem. Phys.*, vol. 142, p. 104703, 2015.
[47] M. Kim, C. W. Joo, J. H. Kim, et al., "Conductivity enhancement of nickel oxide by copper cation codoping for hybrid organic–inorganic light-emitting diodes," *ACS Photonics*, vol. 5, no. 8, pp. 3389–3398, 2018.
[48] A. S. Bhatt, R. Ranjitha, M. S. Santosh, et al., "Optical and electrochemical applications of Li-doped NiO nanostructures synthesized via facile microwave technique," *Materials*, vol. 13, no. 13, pp. 1–17, 2020.
[49] C. Wang, X. Cui, J. Liu, et al., "Design of superior ethanol gas sensor based on Al-doped NiO nanorod-flowers," *ACS Sens.*, vol. 1, no. 2, pp. 131–136, 2016.
[50] Y. J. Mai, J. P. Tu, X. H. Xia, C. D. Gu, and X. L. Wang, "Co-doped NiO nanoflake arrays toward superior anode materials for lithium ion batteries," *J. Power Sources*, vol. 196, no. 15, pp. 6388–6393, 2011.
[51] P. Dubey, N. Kaurav, R. S. Devan, G. S. Okram, and Y. K. Kuo, "The effect of stoichiometry on the structural, thermal and electronic properties of thermally descomposed nickel oxide," *RSC Adv.*, vol. 8, pp. 5882–5890, 2018.
[52] A. Manikandan, J. J. Vijaya, and L. J. Kennedy, "Comparative investigation of NiO nano- and microstructures for structural, optical and magnetic properties," *Physica E Low Dimens. Syst. Nanostruct.*, vol. 49, pp. 117–123, 2013.
[53] Y. Y. Xi, Y. F. Hsu, A. B. Djurišić, et al., "NiO/ZnO light emitting diodes by solution-based growth," *Appl. Phys. Lett.*, vol. 92, no. 11, p. 113505, 2008.
[54] Y. Wang, Q. Niu, C. Hu, et al., "Ultrathin nickel oxide film as a hole buffer layer to enhance the optoelectronic performance of a polymer light-emitting diode," *Opt. Lett.*, vol. 36, no. 8, p. 1521, 2011.
[55] H. H. Gong, X. H. Chen, Y. Xu, F. F. Ren, S. L. Gu, and J. D. Ye, "A 1.86-kV double-layered NiO/β-Ga_2O_3 vertical *p–n* heterojunction diode," *Appl. Phys. Lett.*, vol. 117, p. 022104, 2020.
[56] X. Lu, X. Zhou, H. Jiang, et al., "1-kV sputtered *p*-NiO/*n*-Ga_2O_3 heterojunction diodes with an ultra-low leakage current below 1

μA/cm^2," *IEEE Electron. Device Lett.*, vol. 41, no. 3, pp. 449–452, 2020.
[57] I. López, E. Nogales, B. Méndez, and J. Piqueras, "Resonant cavity modes in gallium oxide microwires," *Appl. Phys. Lett.*, vol. 100, no. 26, pp. 1–4, 2012.
[58] M. García-Tecedor, D. Maestre, A. Cremades, and J. Piqueras, "Tailoring optical resonant cavity modes in SnO_2 microstructures through doping and shape engineering," *J. Phys. D Appl. Phys.*, vol. 50, no. 41, p. 415104, 2017.
[59] J. Bartolome, A. Cremades, and J. Piqueras, "Thermal growth, luminescence and whispering gallery resonance modes of indium oxide microrods and microcrystals," *J. Mater. Chem. C*, vol. 1, no. 41, pp. 6790–6799, 2013.
[60] M. Taeño, D. Maestre, and A. Cremades, "Resonant cavity modes in nickel oxide microcrystals," *Mater. Lett.*, vol. 287, p. 129289, 2021.
[61] M. Taeño, D. Maestre, and A. Cremades, *Fabricación de resonadores ópticos múltiples en el rango visible basados en óxidos metálicos*, Spain, OEPM P202030900, 2020.
[62] J. Geng, Q. Wang, Y. Lee, and S. Jiang, "Development of eye-safe fiber lasers near 2 μm," *IEEE J. Sel. Top. Quant. Electron.*, vol. 20, pp. 150–160, 2014.
[63] M. F. M. Rusdi, A. H. A. Rosol, M. F. A. Rahman, et al., "Q-switched and mode-locked thulium doped fiber lasers with nickel oxide film saturable absorber," *Opt. Commun.*, vol. 447, pp. 6–12, 2019.
[64] B. Sun, Y. Zhang, R. Zhang, et al., "High-order nonlinear optical properties generated by different electron transition processes of NiO nanosheets and applications to ultrafast lasers," *Adv. Opt. Mater.*, vol. 5, no. 8, p. 1600937, 2017.
[65] M. Kumar, T. Som, and J. Kim, "A transparent photonic artificial visual cortex," *Adv. Mater.*, vol. 31, no. 39, pp. 1–8, 2019.